RSC Advances

This is an *Accepted Manuscript*, which has been through the Royal Society of Chemistry peer review process and has been accepted for publication.

Accepted Manuscripts are published online shortly after acceptance, before technical editing, formatting and proof reading. Using this free service, authors can make their results available to the community, in citable form, before we publish the edited article. This *Accepted Manuscript* will be replaced by the edited, formatted and paginated article as soon as this is available.

You can find more information about *Accepted Manuscripts* in the Information for Authors.

Please note that technical editing may introduce minor changes to the text and/or graphics, which may alter content. The journal's standard Terms & Conditions and the Ethical guidelines still apply. In no event shall the Royal Society of Chemistry be held responsible for any errors or omissions in this *Accepted Manuscript* or any consequences arising from the use of any information it contains.

ROYAL SOCIETY OF CHEMISTRY

www.rsc.org/advances

RSC Advances

RSCPublishing

PAPER

Chemical Vapor Infiltration Tailored Hierarchical Porous CNTs/C Composite Spheres Fabricated by Freeze Casting and Their Adsorption Properties

Cite this: DOI: 10.1039/x0xx00000x

Received 00th January 2012,
Accepted 00th January 2012

DOI: 10.1039/x0xx00000x

www.rsc.org/

Junjie Wang[abc], Qianming Gong*[abc], Daming Zhuang[abc] and Ji Liang[d]

Carbon nanotubes (CNTs) were one of the most promising candidates as adsorbents in many fields for their unique structural characters. In this paper, hierarchical porous CNTs/carbon (CNTs/C) composite spheres were prepared and their strength and adsorption of vitamin B12 (VB_{12}) were investigated. The initial porous CNT spheres were fabricated by freeze casting and then followed by freeze drying. Afterwards, the primary porous CNT spheres were further reinforced and tailored by chemical vapor infiltration (CVI) and water steam activation. Consequently, the composite CNTs/C spheres with hierarchical porous structure and high strength were successfully fabricated. SEM and polarized light microscopy observations showed that besides macro-sized radial through-pores in the spheres, lots of micro-sized pores were distributed uniformly in the wall of the radial tunnel like through-pores. Mercury porosimetry and BET tests indicated that the width of the radial lamellar channels was about 5-15 μm and the average diameter of the mesopores was about 3.8 nm. Adsorption of VB_{12} for this hierarchical porous CNTs/C spheres could reach 51.48 mg/g, which was about 3.7 and 3.4 times those of traditional activated carbon beads and macroporous resin beads.

1. Introduction

Carbon nanotubes(CNTs) have aroused great enthusiasm and persistent exploration of applications in many fields over the past years since they were discovered 1991[1]. Thereinto, owing to their relatively high specific surface area and easily modified surface, CNTs have attracted researchers' interests as a promising new sorbent for heavy metals[2-4] in wastewater treatment or for oil slick in rivers or the sea[5,6]. Particularly, based on their meso-porous structure in as-prepared or functionalized powdery CNTs, researchers probed their use for clearing middle molecular toxins in blood as a novel sorbent in hemoperfusion[7]. Both powdery CNTs and CNTs/Carbon composite beads exhibited better performance than traditional sorbents like active carbon beads and macroporous resin beads[8,9].

Obviously, powdery CNTs had many limitations in practical application as sorbents for it was difficult to separate and recycle them from the mixture. Probably this might also cause secondary pollution. Especially, free CNTs must be strictly prohibited in hemoperfusion. So the biggest challenge for taking advantage of CNTs as sorbents was to develop advanced technology to fabricate CNT-based bulk materials. Accordingly, much attention has been paid to the research about syntheses of CNT bulk materials in different shapes such as CNT-fibers[10], CNT-foams[11,12] and 3d-blocks[13,14]. While compared with those bulk materials aforementioned, spherical shaped materials should be more competitive as sorbents or catalyst carrier for their much lower packing density, higher ratio of surface to volume and smaller fluid resistance. Actually, Chao Ye et al. prepared CNTs/phenolic-resin-derived activated carbon beads by spheroidizing small grains of CNTs/phenolic resin in autoclave and found that the adsorption of vitamin B12 (VB_{12}, which was designated as the reference or representative of middle molecular toxins) for the composite beads with 22.5% CNTs was 2.3 times that of commercial macroporous resin[8]. Yuemei Lu et al. increased the ratio of CNTs from 22.5% to 45% in the composite carbon beads by reversed phase suspension polymerization and achieved a high adsorption of low density lipoprotein (LDL) up to 10.46 mg/g[9]. Then reasonably, further increasing the ratio of CNTs in the composite spheres could improve the adsorption capacity of the CNT-based sorbent although it left to be a big challenge. In the mean time, the other concern was that the adsorption capacity of the CNTs far beneath the surface of the composite beads was limited because they were deeply buried and the diffusing channels were limited because in the nearly solid beads, the passageway was mainly developed by steam activation. Undoubtedly, it was hard to get enough accesses from the surface to inner core of the spheres.

Herein the authors proposed a novel strategy to synthesize CNTs/carbon (CNTs/C) composite spheres with high CNT ratio, hierarchical porous structure and high adsorption capacity by combining freezing casting, chemical vapor infiltration(CVI) technology and water steam activation. Freezing casting was a segregation-induced templating of a second phase by solidifying the solvent, which involved preparing a stable suspension, and pouring the suspension into a mould, freezing the suspension then sublimating the solvent

RSC Advances Accepted Manuscript

crystals[15-17]. It was a promising technique to fabricate porous materials with complex pore structure and it has been widely explored in preparing porous ceramic[18,19] and biological materials[20,21]. In this paper, freeze casting was adopted to prepare primary CNTs spheres with radially aligned channels from the core to the surface, and then the brittle pure CNT spheres were strengthened by CVI process during which pyrocarbon was produced to connect or "weld" the adjacent yet discrete CNTs to form integral CNTs/C spheres with high strength. Before adsorption of VB_{12}, water steam activation was fulfilled to improve the hydrophilicity and further tailor the pore structure of the composite spheres.

2. Experimental

2.1 Materials

Multi-walled carbon nanotubes (MWNTs, with the diameter of 10-20 nm and the length of 5-15 μm) were purchased from CNano Technology Ltd. and pre-treated with mixed acid (H_2SO_4:HNO_3 = 3:1) in a reflux condenser for 30 min. The chitosan used as the binder of the initial CNT spheres (degree of deacetylation = 80-95%) and VB_{12} were obtained from Sinopharm Chemical Reagent Beijing Co. Ltd. Acetic acid (A.R., Beijing Chemical Works) was used to dissolve the chitosan. As the contrast, two kinds of typical commercial sorbents, activated carbon(AC) spheres and macroporous resin(MR) spheres were purchased from Aier Hemoperfutor Factory, PR China.

2.2 Preparation of CNTs/C composite spheres

The fabrication process included four steps (Fig.1): i) Mixing the acid pretreated CNTs and chitosan (100:3 in weight ratio) and then dissolving them in 1% acetic acid solution followed by magnetic stirring and further ultrasonic dispersing for 2 hours. ii) Then dripping the uniform suspension into liquid nitrogen dropwise with an injector. Immediately the suspension drop turned into solid beads during the quenching process. After being freeze-dried for 24 h, porous but fragile CNT spheres with a little chitosan binder were obtained. iii) Strengthening the weak spheres in a furnace by CVI process. During this process, pyrocarbon deposited in the interstitial space among CNTs once the mixed gas of C_3H_6 (1 m^3/h) and N_2 (1 m^3/h) infiltrating into the beads at 940 ℃. Although the initial sponge-like freeze-dried CNT spheres were reinforced and some macropores were modified by CVI, some of the nano-sized pores might be blocked somewhat and meanwhile, they became a little hydrophobic after CVI, so the next step was necessary. iv) Activating the CVI reinforced CNTs/C spheres with water steam (0.55 ml/min) by peristaltic pump at 900 ℃ for different time duration. In this process, the pore structure was further tailored and hydrophilic hierarchical porous CNTs/C composite spheres were acquired.

2.3 Characterization

The morphology and microstructure of the samples were investigated with polarized light microscope(PLM) and scanning electron microscopy(SEM)(MERLIN VP Compact, JSM-7001F). Macropores were measured by Mercury porosimetry(AUTO PORE IV 9520) and the pressure range varied between 3.31×10^{-3} and 4.14×10^{2} MPa. The specific surface area, meso- & micro- pores were determined by nitrogen adsorption/desorption at 77 K(Quadrasorb SI-MP) after outgassing at 250 ℃ for 2 h. The BET equation was used to calculate the total specific surface area. The pore distribution and surface area of mesopores were calculated by BJH method. The mechanical property of the spheres was tested in a material testing instrument(Instron 4943) with a 10 N load cell.
The spheres with a uniform diameter of 2.5 mm were placed on the bottom stage and then the top stage was driven down to compress the samples. The loading rate was set as 0.05 mm. min^{-1}.

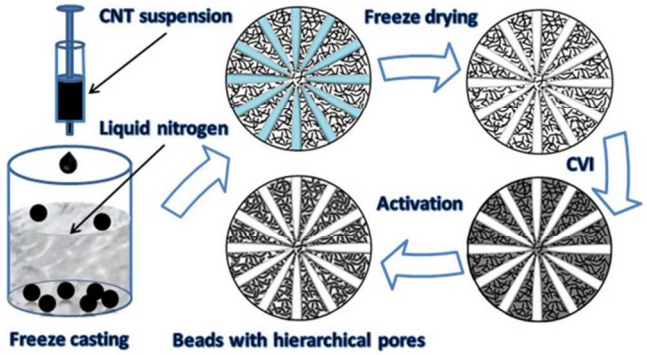

Fig.1 Schematic illustration of the fabrication process of hierarchical porous CNTs/C composite spheres.

2.4 Adsorption of VB_{12}

The adsorption property of the CNTs/C hierarchical porous spheres was evaluated by their adsorption of VB_{12}, the representative of middle molecular toxins. Specifically, 15 mg of the CNTs/C spheres were added into 50 ml of VB_{12} solution (80 mg/L) and the adsorption was carried out in the water bath (37±1 ℃) of a reciprocating shaker at the speed of 150 times per minute for 2 h. An aliquot of the solution was sampled periodically to detect the concentration variation of VB_{12} by using a UV-Vis spectrophotometer at a wavelength of 361±1 nm. The adsorption capacities were calculated as follows:

$$Q_A = \left(\frac{V(C_0 - C_t)}{m}\right) mg.g^{-1}$$

Where Q_A ($mg.g^{-1}$) was the adsorption capacity of VB_{12}, C_0 and C_t ($mg.L^{-1}$) were the concentration of VB_{12} before and after adsorption, V (mL) is the volume of the solution and m (mg) is the weight of the spheres.

3. Results and discussion

3.1 Morphology and microstructure

It was well known that water would turn into ice once the temperature drops below its freezing point. Generally this process is rather slow in nature, while in this study the suspension of CNTs was dripped into liquid nitrogen, the droplets would solidify in no time and so they could keep spherical shape. After freeze drying, spongy CNT spheres with the diameter of 2.5~3 mm were obtained (Fig.2a). Meanwhile, the diameter of the spheres could be adjusted by changing the syringe needles or changing the viscosity of the suspension. Although a little binder was added in case of the spheres collapsed after being freeze dried, the fluffy spheres were quite fragile, so CVI was introduced to reinforce the initial spheres

RSC Advances Accepted Manuscript

This journal is © The Royal Society of Chemistry 2012

since pyrocarbon would deposited preferentially in the interstitial space among CNTs under negative pressure. As a result, the CNTs would be connected or "welded". But CVI time should be controlled in case the pores might be blocked. Actually, the surface of the spheres was full of holes as after CVI (Fig.2b, Fig.2d) and the cross section was consist of radial plate-like structure (Fig.2c). Based on polarized light microscope images (Fig.2e), it could be discerned that the cross section was composed of radial laminar pores which were developed directionally from the surface to the inner core. The wall thickness of the pores was about 1 μm and the width of the laminar pores was about 5~15 μm (inlet of Fig.2e). But it must be pointed out that the alignment of laminar structure varied a little especially in the outer layer of the spheres, i.e., some zones were built by laminar pores parallel perfectly with each other (Fig.2h) while others were composed of domains in which the orientation of the pore walls were different (Fig.2f). Adjacent to the outer layer, laminar pores were well aligned radially from the center. This radial microstructure should have something to do with the ice crystal growth during solidification process since the growth rate along different lattice plane was not equivalent (inlet of Fig.2g) and it would be discussed in the next section.

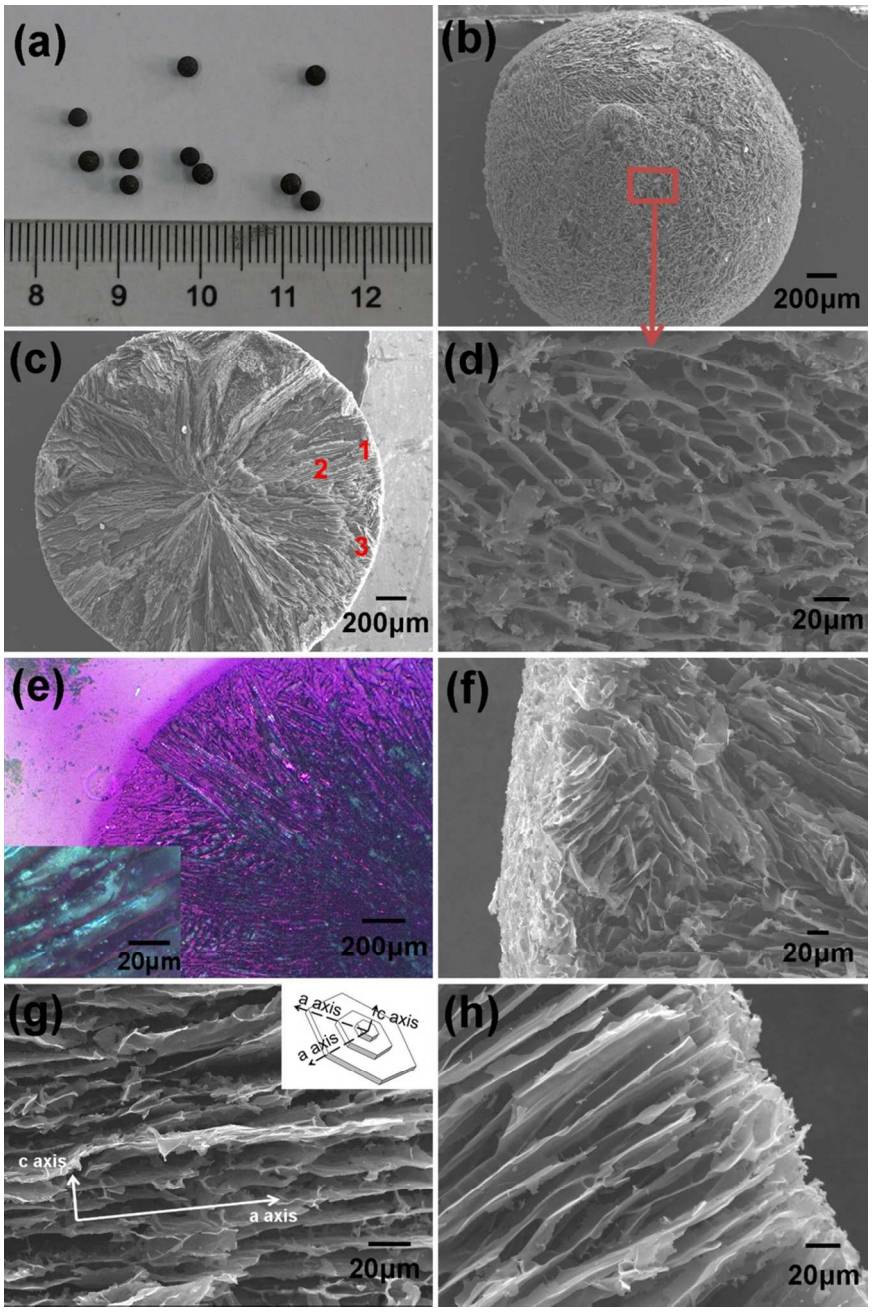

Fig.2 Optical photograph of CNTs/C composite spheres (a), SEM images of the surface (b), cross section (c), magnified surface morphology (d), PLM image of the cross section (e), zoomed in microstructure of framed area 1(f), framed area 2(g) and framed area 3(h). (Note: Inlet in Fig.2e was the magnified detailed view of laminar structure and the one in Fig.2g was the schematic crystal lattice of ice.)

RSC Advances Accepted Manuscript

RSC Advances RSCPublishing

PAPER

Different from traditional activated carbon beads, in which mainly micropores were developed by activation in the surface layer and almost no passageway to center existed, the CNTs/C spheres had a lot of radial pores which could play as the straightway channels for the diffusivity of solutions. Besides, in the spheres there existed abundant mesopores which were crucial for adsorption of middle molecular matters. Generally, before CVI process, the mesopores in the fluffy CNT spheres were mainly resulted from the loose aggregation or stacking of CNTs in the walls of the tunnels (Fig.3a)[7] and they would be further quantified by N_2 adsorption tests.

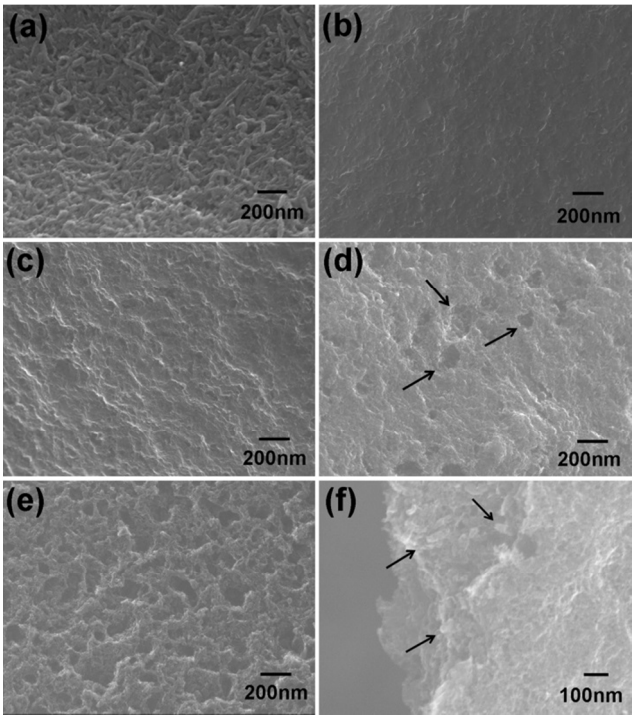

Fig.3 SEM micrographs of the channel walls of the freeze-dried spheres (a), after CVI for 4 h (b), after being activated by water steam for 30 min (c), for 45 min (d), for 60 min (e) and CNTs in fractured surface of the channel walls (f).

The hierarchical pore structure of the spheres should be favorable for adsorption, nevertheless, the maximum load of the sponge spheres was only 0.135 N. Basically, pyrocarbon would preferentially deposited in the nano-sized interstitial space between two carbon nanotubes. Hence theoretically, an appropriate ratio of pyrocarbon could just connect adjacent CNTs to strengthen the fragile spheres yet it would not block the initial pores. While after CVI for 4 h, the channel walls were coated with pyrolytic carbon homogeneously (Fig.3b). Although the pyrocarbon film could significantly increase the strength of the spheres to 2.231 N, some of the meso- and micro-pores were blocked. Thus, further activation was necessary for recovering and further tailoring the pore structure. 30 min of activation made the wall surface rough (Fig.3c) and afterwards, some etched pits of about 50~100 nm in diameter produced when extending activation to 45 min (Fig.3d). Once further increasing activation time to 60 min, more pits appeared and some got enlarged (Fig.3e). In the mean time, CNTs came to expose again (Fig.3e,3f) and predictably, the specific surface area and pore volume would be improved greatly in the hierarchical porous CNTs/C spheres.

3.2 Pore structure evolution

Usually, the pore structure of traditional activated carbon beads was developed mostly at the stage of activation and by contrast, the hierarchical porous structure of CNTs/C spheres was primarily determined by freeze casting, and then tailored further by CVI and water steam activation during which pore structure and strength was modified to match up preferably. Thus a deep understanding of the pore structure evolution was favorable to take full advantage of the adsorption capacity of CNTs to the great extent.

More specifically, at the initial stage of freeze casting, once the CNT suspension was dropped into the liquid nitrogen, the temperature of the thin surface layer decreased to -196 ℃ instantly and the temperature at the center remained as room temperature. This process could be simulated by finite element analyses (Fig.4a), and then in less than 3 seconds, the outer layer got frozen (Fig.4b). Since the degree of supercooling in the outer layer was much higher than that necessary for water freezing, a large amount of ice nuclei generated simultaneously. Correspondingly, this homogeneous nucleation brought about randomly aligned polycrystalline structure. Whenever the outer layer transformed into ice, the heat inside could only be conducted radially via ice and the temperature gradient decreased greatly. Then the radial aligned temperature distribution would definitely lead to radial ice crystals.

As one of the 15 known crystalline phases of ice, the hexagonal lattice shown in Fig.2g was the most common structure. According to the research of Deville et al, the chemical potential of the ice crystal was different in different crystal planes. The facets parallel to c axis had a higher chemical potential than the ones parallel to a axis and thus the ice growth rate along the a axis was 10^2-10^3 times faster than that along the c axis. Accordingly, when the temperature gradient parallelled to a axis of the crystal, the crystal would have a kinetically favorable condition to grow up into a lamellar structure[22-25]. Of course, between the thin outer layer of randomly aligned domains and the inner layer regular radial structure, there should be a transitional zone which connected the two parts (Fig.2e). After being freeze dried, the ice crystals were sublimed and the evolved pores were just exactly the mirror image of the ice crystals. As a whole, the pore structure (Fig.2) was in fairly consistent with the above theoretical analyses.

To determine the size and distribution of radial macro-channels, mercury (Hg) intrusion method was adopted to analyze the CNTs/C spheres. The results in Fig.5 indicated that the median pore diameter was 9.20 μm and most of the macro-pores was in the diameter of 6~12 μm, which were quite consistent with the

RSC Advances Accepted Manuscript

observations by SEM and PLM (Fig.2). Reasonably, the size, morphology and distribution of the macro-channels could be designed and fabricated under control and this interesting work being carried on would be discussed in the future.

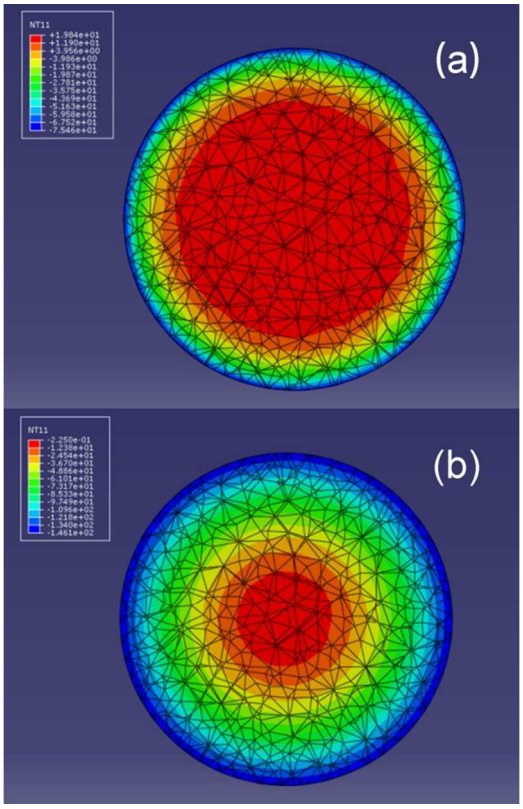

Fig.4 Finite element simulation diagram of the temperature distribution along the cross section after the suspension of CNTs being dropped in liquid nitrogen for 0.47 s (a) and 2.61 s (b).

Fig.5 Macro-pore test of the freeze dried CNT spheres by mercury porosimetry

As absorbents for middle molecular matter, mesopores that were scarce in traditional activated carbon beads were indispensible. In this work, the initial mesopores among intertwined CNTs might be blocked a little during CVI process and then in the following activation process, the pore structure would be tailored and developed further. The pore structure evolution was monitored by BET tests (Fig.6, Table1)

It could be noted that in Fig.6a, the N_2 adsorption-desorption isotherm of the freeze dried spheres had the typical character of type IV curve which were in accordance with the mesoporous structure of loosely stacking CNTs[7]. Although CVI reinforced the fragile freeze dried spheres, it might cause the blockage of some of the meso- and micro-pores, while after further activated by water steam, the filmy pyrocarbon would be etched away and some micropores might be developed to be mesopores. So the total pore volume would be increased with the extension of activation time (Fig.6a). After being activated for 60 min, the pore volume and specific surface area of the sample were higher than that of initial freeze dried CNT spheres. By contrast, even the total BET specific surface area and total volume were much higher for AC beads and MR beads, the mesopore volumes of these two were approximately equal to that of activated CNTs/C spheres. Nevertheless, the average pore diameters of AC beads and MR beads were only about 1.4 nm, which was much lower than that of CNTs/C spheres. In addition, it could be confident that if more work being carried out on modifying the proportion of pyrocarbon and CNTs followed by controlling the degree of activation, a higher ratio of mesopores could be acquired. As adsorbents, besides pore volume, pore size and distribution were the other key factors as well. It was interesting that the pore size distribution of the original spheres and activated ones were quite similar (Fig.6b) The average pore diameters of all the samples were almost equal to 3.8 nm. Probably, the mesopores in the stacking CNTs were kept all the way even though the pore evolution process was complicated.

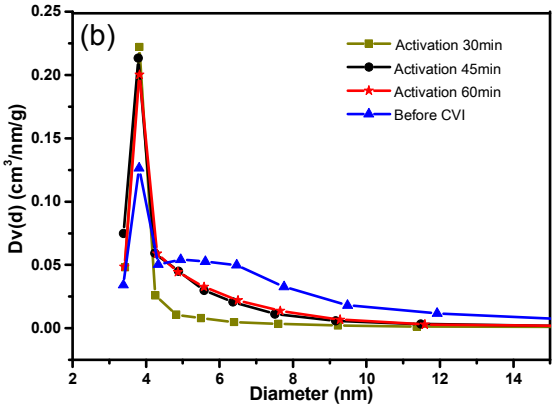

Fig.6 Pore structure character analyzed by N_2 adsorption-desorption isotherms (a) and pore size distribution of the porous spheres (b).

RSC Advances Accepted Manuscript

Table1 Pore diameters, volumes and BET specific surface areas of CNTs/C spheres, AC and MR beads

Samples	Average pore diameter (nm)	Mesopore volume (cm^3/g)	Total pore volume (cm^3/g)	Mesopore specific surface area (m^2/g)	Total BET surface area (m^2/g)
Original CNT spheres	3.781	0.217	0.255	193.747	218
Activated CNTs/C (30)	3.820	0.133	0.153	115.629	174
Activated CNTs/C (45)	3.791	0.240	0.297	188.973	257
Activated CNTs/C (60)	3.820	0.253	0.287	195.774	280
AC beads	1.418	0.255	0.557	63.620	810
MR beads	1.439	0.241	0.702	119.78	961

3.3 VB_{12} adsorption

As the representative of middle molecular toxins in hemoperfusion, VB_{12} was always adopted to evaluate the adsorption capacity of new adsorbents. Currently, AC beads and MR beads have been applied in hemoperfusion for years. In contrast, the adsorption of VB_{12} in 2 h at 37 ℃ for AC beads was 13.98 mg/g and that for MR beads was 15.25 mg/g, which were a little higher than that for CNTs/C spheres activated for 30 min. With the increase of activation time, the adsorption capacity of CNTs/C spheres was improved greatly. The sample activated for 60 min had an adsorption of 51.48 mg/g, which was 3.68 times as that of AC beads and 3.38 times that of MR beads (Fig.7a). Moreover, adsorption rate of CNTs/C spheres was much higher than that of AC beads and MR beads (Fig.7b). Albeit functional groups should be similar for CNTs/C spheres and AC beads due to the similar water steam activation process, their pore structures were quite far from each other. Mesopores with the diameter of more than 2 nm might be one of the prerequisites for adsorbing VB_{12} for the size of VB_{12} was about 2.09 nm. Although the total pore volume and total BET specific surface area of AC beads and MR beads were rather higher than those of CNTs/C spheres, mesopore volumes of the two control samples were nearly equal to that of activated CNTs/C spheres, then it should be reasonable to deduce that it was not the mesopores, but the micropores in AC beads and macropores in MR beads that contributed to the relatively higher values of total pore volumes and total specific surface areas. Moreover, unfavorably, most of the pore diameters in AC beads and MR beads were lower than that of VB_{12}.

Therefore, besides the advantages in mesopore diameter, mesopore volume and mesopore specific surface area for CNTs/C spheres listed in Table 1, the highly developed radial aligned macro-channels could play the other key role as the diffusing throughway for VB_{12} solution. That was why the adsorption capacity of CNTs could be taken fully utilized in the spheres. In addition, the mesopores built in walls of radial channels could accelerate the adsorption rate. Hopefully, this hierarchical porous CNTs/C spheres could be a potential candidate in hemoperfusion or other related fields.

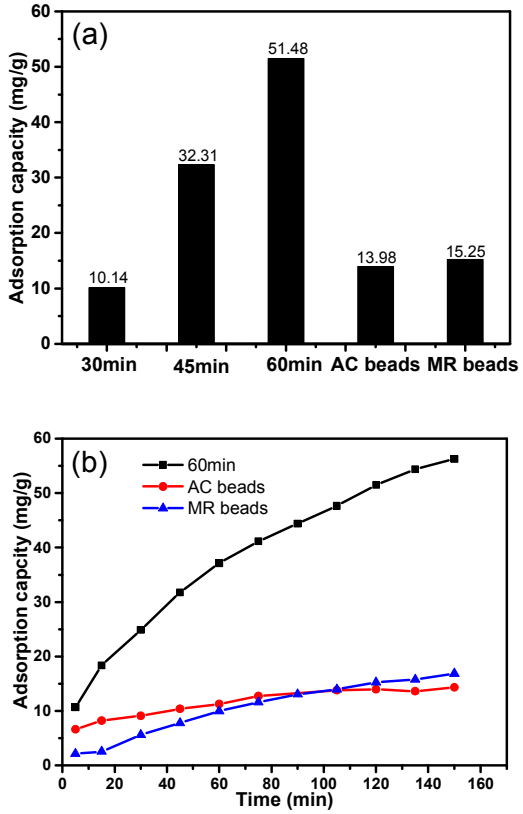

Fig.7 Adsorption capacity in 2 h (a) and adsorption rate (b) for VB_{12} by CNTs/C spheres, AC beads and MR beads.

3.4 Mechanical properties

The initially freeze dried green CNT spheres were rather brittle and they tended to fall apart during the adsorption tests in shaker due to the weak connection among CNTs. Obviously the green CNT spheres were not suitable to be used as adsorbents directly for they might bring about secondary pollution. After CVI for 4 h, the mass gained 45.63% and the breakage force of the CNTs/C spheres was greatly improved from 0.135 N of the green CNT spheres to 2.231 N. The maximum breakage load was 15.53 times higher than that of the green CNT spheres (Fig.8). While inevitably, some micro- and meso-pores might be blocked somewhat and that would be unfavorable for

RSC Advances Accepted Manuscript

This journal is © The Royal Society of Chemistry 2012

adsorption. To compromise this contradiction, water steam activation should be taken to acquire an optimal combination of the strength and adsorption capacity.

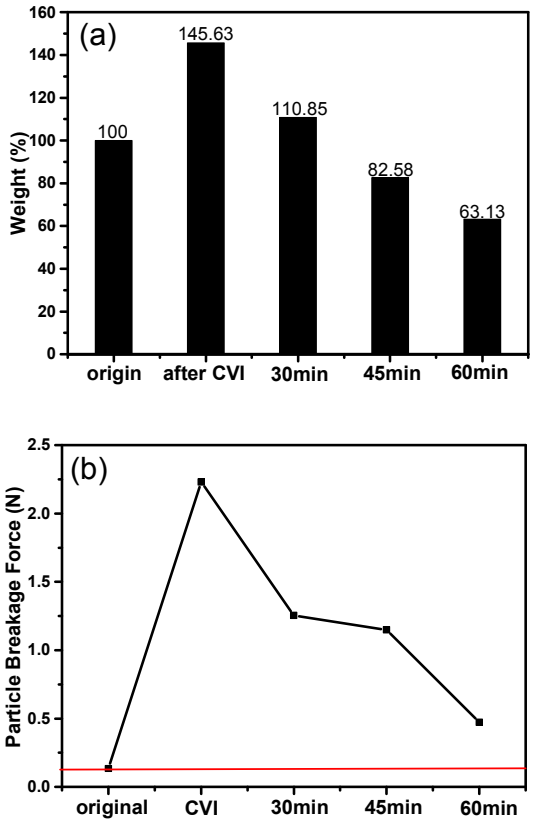

Fig.8 The mass variation of the spheres after CVI and being activated for different time (a) and breakage forces of the corresponding spheres (b). (Note: the mass of the initial CNT spheres were recorded as 100%, 30 min meant being activated for 30 min and so on)

In Fig.8a, it could be figured out that after CVI, the mass gain was 45.63%, which implied that the mass ratio of CNTs and pyrocarbon was about 2:1. During activation, the burn-offs became larger with increasing time and the mass of 30 min activated samples was still 10.85% higher than the green CNT spheres, but it was difficult to discern whether the pyrocarbon or CNTs, or both that should be responsible for the mass loss. Whatsoever, after being activated for 45 min or more, the mass was lower than the initial spheres. While fortunately, the breakage forces were still much higher than that of the initial ones (Fig.8b), even for the 60 min activated ones, which was about 37% mass loss compared with the initial ones. This indicated that both CNTs and pyrocarbon would be etched if being activated for certain time duration. Since the breakage force of 45 min activated sample (1.148 N) was only a little lower than that of 30 min activated one (1.254 N), adsorption capacity of the former was 3.2 times that of the latter and thus probably, 45 min activation might be applicable.

4. Conclusion

In this paper, CNTs/C composite spheres with special hierarchical porous structure were prepared successfully in a novel way. The radial laminar channels from the center to the surface were formed during freeze casting process which could act as the throughway for the solution diffusivity. The mesopores in the channel walls were tailored by the subsequent CVI and water steam activation process. The width of the lamellar channels was about 5-15 μm and the average diameter of the mesopores was about 3.8 nm. In addition, the breakage load for the primary CNT spheres could be improved from 0.135 N to 2.231 N after CVI reinforcing process although it might decrease a little after activation. As a promising adsorbent, the adsorption capacity of the CNTs/C composite spheres for VB_{12} was about 51.48 mg/g, which was 3.7 and 3.4 times those of traditional AC beads and MR beads and moreover, the adsorption rate was also higher than the other two referential samples. The excellent adsorption properties should be attributed to the hierarchical porous structure of the composite spheres. Further, microstructure and finite element analyses indicated that the pore structure could be designed and modified in a more accurate way by controlling the suspension concentration, freeze casting, CVI duration and activation process and this deserved further studying.

Acknowledgements

The authors would like to thank Prof. Haiyan Zhao and Prof. Zhipeng Cai in Tsinghua University for their help in finite element analyses.

[a] Key Laboratory for Advanced Materials Processing Technology, Ministry of Education, Beijing 100084, P. R. China
[b] School of Materials Science and Engineering, Tsinghua University, Beijing 100084, P. R. China
[c] State Key Laboratory of New Ceramics and Fine Processing, Tsinghua University, Beijing 100084, P. R. China
[d] Department of Mechanical Engineering, Tsinghua University, Beijing 100084, P. R. China
*Corresponding author. Email: gongqianming@mail.tsinghua.edu.cn.

References

1 Iijima S. Helical microtubules of graphitic carbon, *Nature*, 1991, **354**(6348), 56-58.
2 Xianjia Peng, Zhaokun Luan, Zechao Di, Zhongguo Zhang, Chunlei Zhu, Carbon nanotubes-iron oxides magnetic composites as adsorbent for removal of Pb(II) and Cu(II) from water, *Carbon*, 2004, **43**(4), 880-883.
3 Munther Issa Kandaha, Jean-Luc Meunier, Removal of nickel ions from water by multi-walled carbon nanotubes, *Journal of Hazardous Materials*, 2007, **146**(1-2), 283-288.
4 Sahika Sena Bayazita, Ismail Incib, Adsorption of Pb(II) ions from aqueous solutions by carbon nanotubes oxidized different methods, *Journal of Industrial and Engineering Chemistry*, 2013, **19**(6), 2064-2071.
5 Daniel P. Hashim, Narayanan T. Narayanan, Jose M. Romo-Herrera, David A. Cullen, Myung Gwan Hahm, Peter Lezzi, Joseph R. Suttle, Doug Kelkhoff, E. Munoz-Sandoval, Sabyasachi Ganguli, Ajit K. Roy, David J. Smith, Robert Vajtai, Bobby G. Sumpter, Vincent

RSC Advances Accepted Manuscript

Meunier, Humberto Terrones, Mauricio Terrones & Pulickel M. Ajayan, Covalently bonded three-dimensionalcarbon nanotube solids via boroninduced nanojunctions, *Nature*, 2012, **2**(363), 1-8.

6 Xuchun Gui, Zhiping Zeng, Zhiqiang Lin, Qiming Gan, Rong Xiang, Yuan Zhu, Anyuan Cao, and Zikang Tang, Magnetic and Highly Recyclable Macroporous Carbon Nanotubes for Spilled Oil Sorption and Separation, *ACS Appl. Mater. Interfaces*, 2013, **5**(12), 5845-5850.

7 Chao Ye, Qian-Ming Gong, Fang-Ping Lu, Ji Liang, Adsorption of uraemic toxins on carbon nanotubes, *Separation and Purification Technology*, 2007, **58**(1), 2-6.

8 Chao Yea, Qian-Ming Gong, Fang-Ping Lub, Ji Liang, Preparation of carbon nanotubes/phenolic-resin-derived activated carbonspheres for the removal of middle molecular weight toxins, *Separation and Purification Technology*, 2008, **61**(1), 9-14.

9 Yuemei Lu, Qianming Gong, Fangping Lu, Ji Liang, Preparation of sulfonated porous carbon nanotubes/activated carbon composite beads and their adsorption of low density lipoprotein, Separation and Purification Technology, *Journal of materials science materials science materials in medicine*, 2011, **22**(8), 1855-1862.

10 Mei Zhang, Ken R. Atkinson, Ray H. Baughman, Multifunctional Carbon NanotubeYarns by Downsizing an Ancient Technology, *Science*, 2004, **306**(5700), 1358-1361.

11 Mei Zhang, Shaoli Fang, Anvar A. Zakhidov, Sergey B. Lee, Ali E. Aliev, Christopher D. Williams, Ken R. Atkinson, Ray H. Baughman, Strong, Transparent, Multifunctional, CarbonNanotube Sheets, *Science*, 2005, **309**(5738), 1215-1219.

12 Rajib K. Das, Bo Liu, John R. Reynolds, Andrew G, Rinzler, Engineered Macroporosity in Single-Wall Carbon Nanotube Films, *Nano Letters*, 2009, **9**(2), 677-683.

13 Jianhua Zou, Jianhua Liu, Ajay Singh Karakoti, Amit Kumar, Daeha Joung, Qiang Li, Saiful I. Khondaker, Sudipta Seal, and Lei Zhai, Ultralight Multiwalled Carbon Nanotube Aerogel, *ACS Nano*, 2010, **4**(12), 7293-7301.

14 Xuchun Gui, Jinquan Wei, Kunlin Wang, Anyuan Cao, Hongwei Zhu, Yi Jia, Qinke Shu, and Dehai Wu, Carbon Nanotube Sponges, *Advanced Materials*, 2010, **22**(5), 617-621.

15 Sylvain Deville, Ice templating, freeze casting: Beyond materials processing, *Journal of Materials Research*, 2013, **28**(17), 2202-2219.

16 E. Munch, J. Franco, S. Deville, P. Hunger, E. Saiz, and A.P. Tomsia, Porous Ceramic Scaffolds with Complex Architectures, *Biological Materials Science*, 2008, **60**(6), 54-58.

17 Sylvain Deville, Eduardo Saiz , Antoni P. Tomsia, Ice-templated porous alumina structures, *Acta Materialia*, 2007, **55**(6), 1965-1974.

18 Florian Bouville, Eric Maire, Sylvain Deville, Lightweight and stiff cellular ceramic structures by ice templating, *Journal of materials Research*, 2013, **29**(2), 175-181.

19 Ming-Hua Ho, Pei-Yun Kuo, Hsyue-Jen Hsieh, Tzu-Yang Hsien, Lein-Tuan Hou, Juin-Yih Laid, Da-Ming Wang, Preparation of porous scaffolds by using freeze-extraction and freeze-gelation methods, *Biomaterials*, 2004, **25** (1), 129–138.

20 Ulrich Soltmanna, Horst Bo¨ttcher, Dietmar Koch, Georg Grathwohl, Freeze gelation: a new option for the production of biological ceramic composites (biocers), *Materials Letters*, 2003, **57**(19), 2861-2865.

21 K. M. Pawelec, A. Husmann, S. M. Best and R. E. Cameron, A design protocol for tailoring ice-templated scaffold structure, *journal of the royal society interface*, 2014, **11**(92), 1-9.

22 W. L. Li, K. Lu and J. Y. Walz, Freeze casting of porous materials: review of critical factors in microstructure evolution, *International Materials Review*, 2012, **57**(1), 37-60.

23 Sylvain Deville, Freeze-Casting of Porous Ceramics: A Review of Current Achievements and Issues, *Advanced Engineering Materials*, 2008, **10**(3), 155-169.

24 Sylvain Deville, Eric Maire, Audrey Lasalle, Agne`s Bogner, Catherine Gauthier, Jerome Leloup, and Christian Guizard, In Situ X-Ray Radiography and Tomography Observations of the Solidification of Aqueous Alumina Particle Suspensions—Part I: Initial Instants, *Journal of the American ceramic society*, 2009, **92**(11), 2489-2496.

25 Sylvain Deville, Eric Maire, Audrey Lasalle, Agne`s Bogner, Catherine Gauthier, Jerome Leloup, and Christian Guizard, In Situ X-Ray Radiography and Tomography Observations of the Solidification of Aqueous Alumina Particle Suspensions—Part II: Initial Instants, *Journal of the American ceramic society*, 2009, **92**(11), 2497-2503.

RSC Advances Accepted Manuscript

 This journal is © The Royal Society of Chemistry 2012